Experimental Studies of Heterogeneous Nucleation in the Turbulent Mixing Condensation Nuclei Counter

Rashid Mavliev,[†] Philip K. Hopke,*[,‡] Hwa-Chi Wang,[†,§] and Doh-Won Lee[‡]

Illinois Institute of Technology, Chicago, Illinois 60616, Clarkson University, Potsdam, New York 13699-5708, and Air Liquide, Chicago Research Center, Countryside, Illinois 60525

Received: August 1, 2003; In Final Form: December 26, 2003

A method for varying the supersaturation in a turbulent mixing CNC has been used to examine heterogeneous nucleation of different compounds (working fluid) on various nuclei's compositions. Supersaturation was controlled by changing the vapor pressure of working fluid in nozzle flow, which was accomplished by saturating only a predetermined fraction of the flow while the keeping the total flow and temperature constant. This approach allows the partial pressure of the working fluid to be varied while maintaining a constant flow structure and temperature field. Experimental results characterizing the initial stages of heterogeneous nucleation are presented for NaCl, KCl, AgCl, and Ag particles. Heterogeneous nucleation was examined at various pressures of dibutylphthalate, octadecane, octadecanol, and octadecanoic acid. For octadecanoic acid as the working fluid, the size distribution of the grown particles is unimodal with the size increasing with increasing pressure of the working fluid. For the other working fluids, the initial size distribution splits into a bimodal distribution with one mode approximately the same as the initial distribution and a larger sized mode that grows with increasing pressure of the condensing vapor. For NaCl and octadecane and octadecanol, the initial unimodal size distribution splits into a trimodal size distribution.

Introduction

Ultrafine particles (particles with diameters <100 nm) play an important role in atmospheric processes such as cloud formation, and thus in indirect effects on the albedo and the radiation balance, and ozone depletion. They dominate the number concentrations in the atmosphere. One of the major hypotheses that has been proposed for the cause of the observed effect of particulate matter on health is that high numbers of ultrafine particles (diameters less than 0.1 μm) rather than particle mass are responsible for the adverse health effects. The health effect of ultrafine particles also became a concern in recent years.[1] Wichmann et al.[2] found significant associations of elevated cardiovascular and respiratory disease mortality with various fine (and ultrafine) particle indices evaluated in Erfurt, Germany. Significant associations were found between mortality and ultrafine particle number concentration (NC), ultrafine particle mass concentration (MC), fine particle mass concentration, or SO_2 concentration. The correlation between MC in the 0.01−2.5 μm size range and NC in the size range of 0.01−0.1 μm is only moderate, suggesting it may be possible to partially separate effects of ultrafine and fine particles. Thus, measurements of the ultrafine particle concentrations as well as particle mass are needed to help provide more data to examine these relationships. Such measurements then depend on reliable systems to count the particles. The usual measurement system is a condensation nuclei counter (CNC) in which a working fluid is condensed onto the particle such that it grows to a size where it can effectively scatter light and be detected.

The effectiveness of the nucleation and growth processes in activating particles of different compositions is critical to the performance of a CNC. Thus, the investigation of the effects of the nuclei composition and working fluid on nucleation activation is important. However, very little information is available in the literature. Helsper and Neissner[3] investigated the effect of the vapor substance on the behavior of the expansion type CNC for water and butanol. They found that particle substance (Ag and NaCl) did not affect the Kelvin diameter when butanol was used as the working fluid. However, the size of NaCl particles was overestimated by 2.5 times when water was used. Similar results were found in the work of Porstendörfer et al.[4] Kousaka et al.[5] found less profound but still different results for NaCl and Ag particles. Limited results presented by Madelaine and Metayer[6] showed an essential difference on CNC sensitivity for NaCl, V_2O_5, and H_2SO_4 particles. Holländer et al.[7] have examined the nucleation of a number of working fluids and find that only *n*-butanol and tetrachloroethylene were effective in detecting laboratory-generated graphite particles. This preliminary information confirms the influence of the nuclei and the working fluid properties.

Limited experimental data are available on the nucleation of model compounds onto particles of various compositions to examine the relationship between molecular properties of the condensing vapor (working fluid) and the particles. Kulmala et al.[8] have examined the nucleation of water−*n*-propanol and water−sulfuric acid mixtures on 9, 90, and 900 nm silver particles by determining the onset vapor pressures for nucleation when there is growth of the resulting droplet up to sizes that effectively scatter light. Chen and co-workers[9−12] have performed a series of studies of nucleation of water and *n*-butanol onto various composition particles (SiO_2, TiO_2, glucose, lactose, and monosodium glutamate) using a flow diffusion cloud

* To whom correspondence should be addressed. E-mail: hopkepk@clarkson.edu.
[†] Illinois Institute of Technology.
[‡] Clarkson University.
[§] Air Liquide, Chicago Research Center.

10.1021/jp0362537 CCC: $27.50
Published on Web 03/12/2004

chamber. They also studied the supersaturation values at which nucleation and growth to large droplets occur and examine particle sizes in the range of 15−20 nm. They found that the experimental critical supersaturation values were smaller than were predicted by the Fletcher version of classical nucleation theory. Hogrefe and Keese[13] examined the nucleation of water on glass spheres and again measured the critical supersaturation values for large particles (4 μm diameter). This study suggested a strong influence of surface properties of the individual particles. These studies generally were only able to study particles that experienced nucleation and growth to sufficiently large sizes to permit effective Mie scattering. The details of the activation and growth were not examined.

Currently, the theoretical understanding of heterogeneous nucleation is limited and additional data characterizing the nucleation process should provide useful insights into the nature of the processes involved. Thus, a program of measurements has been undertaken to determine the nature of condensation of working fluids of different molecular properties on different composition nuclei. Prior work concentrated on nucleation on ultrafine carbon particles.[14] In this study, other composition particles are studied.

Background

Lee et al.[14] present a detailed description of classical heterogeneous nucleation theory. Classical theory represents an ideal situation where the details of the interaction of the nuclei with the condensing vapor molecules are parametrized in the contact angle between the forming droplet and the surface of the nucleus. Such a simplification can be expected to be adequate when the nuclei and the condensing vapor are the same material or when the nuclei are insoluble but have a surface that is completely wettable by the condensable vapor. However, the interaction between the nuclei and vapor molecules and the heterogeneity of the nucleus' surface can be expected to have a strong influence on the heterogeneous nucleation process. The equations relating the Kelvin diameter with the supersaturation ratio are simplified cases of heterogeneous nucleation. If the particle is not perfectly wetted by the fluid, the situation becomes more complicated. The energy of the formation of the critical embryo will involve the interaction of solid−liquid and liquid−gas interfaces. In real situations, the interaction between the vapor and particles is not well-known, especially for particles of unknown composition such as those that are present in the ambient atmosphere.

The goal of present study is to examine the early stages of heterogeneous nucleation using a recently developed technique for supersaturation scanning in a CNC and using a DMA capable of operating in nanometer size range to measure the resulting particle size distributions.

Experimental System

The experimental system is shown schematically in Figure 1. The basic components are the particle generators, the condensation nuclei counters (CNC), and a differential mobility analyzer (DMA). The turbulent mixing condensation nuclei counter (TMCNC) has been previously described.[14,15] These components will be described in the subsequent subsections.

Particle Generation. Four different types of particles, NaCl, KCl, Ag, and AgCl, were used in the experiments. The physical and chemical parameters of substances used for particle generation are presented in Table 1. Particles were generated by evaporation in a high-temperature furnace and subsequent cooling of the vapor by mixing it with a cold flow. This method

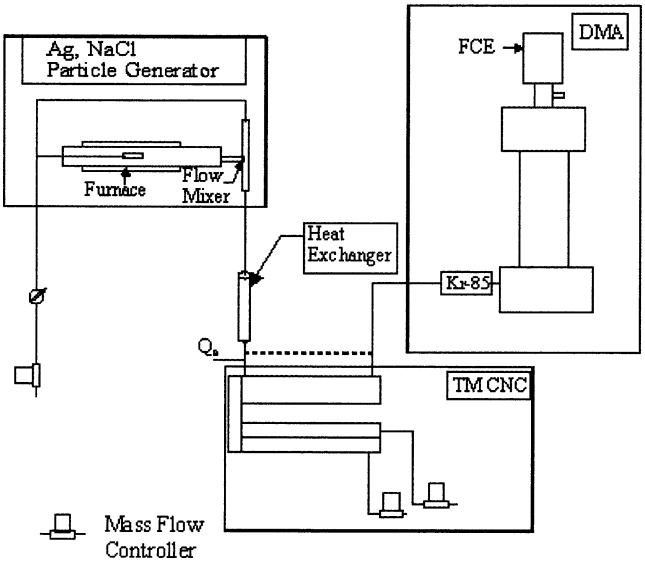

Figure 1. Schematic diagram of the experimental setup. Vienna type differential mobility analyzer (DMA), Faraday cup electrometer (FCE), turbulent mixing CNC (TMCNC), aerosol charger Kr-85 (TSI).

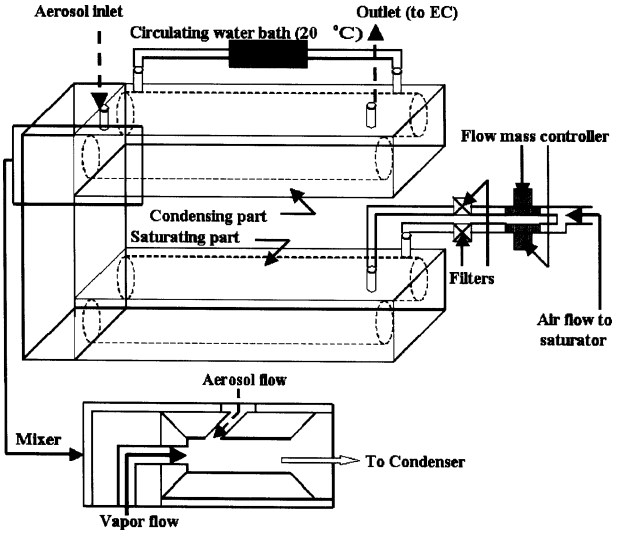

Figure 2. Scheme of modified turbulent mixing CNC.

TABLE 1: Physical and Chemical Parameters of Substances Used for Particle Generation

substance	molecular weight	edge length (nm)	crystal structure	generator temp (° C)	vapor flow (lpm)
NaCl	58.45	0.564	BCC	600−608	0.05−0.15
KCl	74.55	0.629	BCC	640	0.37−0.47
Ag	107.87	0.409	FCC	1125−1140	0.7
AgCl	143.34	0.555	BCC	530	1.1

allows particle generation in the size range of 2−20 nm. Working temperatures are shown in the Table 1. The experimental system was arranged to allow a quick change from one type of particles to another without disturbing the DMA and CNC operating parameters. This flexibility allowed the investigation of heterogeneous nucleation for several substances under very similar conditions. Typically, NaCl particles were used as a reference.

Condensation Nuclei Counter. A schematic diagram of the modified TMCNC is shown in Figure 2 and consists of three major parts−saturator, mixer and condenser. All three parts of TMCNC are machined from blocks of aluminum alloy. The flow channels are machined by drilling through the aluminum block.

Additional holes are drilled to install the heating elements and solid-state temperature sensors. This approach allows uniform temperature distribution within the block.

The vapor generator (saturator) and mixer are placed in an outer Teflon shell for insulation up to 150 °C. Temperatures of these two parts are controlled separately by a circuit board and a data acquisition system (5500MF from ADAC Corp.) with an accuracy of ±0.1 °C. Two chambers of equal size with volumes of approximately 80 cm^3 were machined in the saturator block. The aluminum alloy crucibles can be filled with 15−20 cm^3 of working fluid to saturate the flow with the working fluid vapor ("wet" side). Another chamber is kept empty and is then always dry ("dry" side). Flows from these two chambers are connected and mixed in the mixing chamber (see Figure 2) before passage through an expansion nozzle to the condenser. Together these two flows constitute the "hot" flow in the system.

The degree of supersaturation is adjusted by varying the ratio of flows passing through these two chambers that are equilibrated at the same temperature. The saturated vapor flow is directed to the condenser through a 1 mm diameter nozzle. The aerosol or "cold" flow is directed into the condenser through a circular opening. These two coaxial flows are mixed and directed through an outlet connector to the particle detection system. The residence time of particles in the condenser is about 1.9 s assuming fully developed flow in the condenser. The condenser is cooled by a circulating water bath at temperatures in the range of 10−20 °C to permit subsequent condensation. The size distribution and the concentration of particles after condensational growth is examined with a differential mobility analyzer (DMA).

Differential Mobility Analyzer. A Vienna-type DMA (HAUKE, Vienna, Austria) was used for particle classification in the size range below 50 nm.[16] Recent studies on the selection efficiency of this system show that proper adjustment of the sample/sheath flow ratio allows an attainment of 5% resolution at the high end and 10% at the low end for sizes ~1 nm.[17] At the sample and sheath flows used in these experiments (3 lpm and 28 lpm, respectively), the width of the transfer function should be approximately 12%, but because of the effect of diffusion broadening in the small particle range, the real width can reach 20%.[18,19] An aerosol electrometer was used to detect the particles that are transmitted through the DMA. During the experiments, the DMA was used in scanning mode (typically 43 channels). Measurement data was processed by DMA software to obtain the size distribution of particles. The integrated data processing software allows the probability of charging and multiple charge effects[20] to be taken into account. As part of the DMA, a radioactive source of ^{85}Kr was used to impart a low charge distribution. A concern in these experiment was the potential production of particles through ion-induced nucleation. The ^{85}Kr source was used because earlier work had suggested it was less likely to produce additional particles.[21]

Supersaturation Scanning. Supersaturation scanning in the TMCNC is achieved by changing the initial pressure of the working fluid in the "hot" flow. The carrier gas to the vapor generator (0.8 lpm or 1 lpm) is split into two flows (wet and dry) at the entrance. These two flows are recombined inside the mixing chamber before being directed to the nozzle. This approach permits changing the initial working fluid pressure in the vapor generator flow by changing the ratio of flows through "wet" and "dry" chambers while keeping the flow structure and the temperature field unchanged.[14,15]

Properties of Working Fluids. Four working fluids, dibutylphthlate, octadecane, octadecanol, and octadecanoic acid, were used and physical chemical parameters are given in Table 2. These compounds were chosen to be similar in their thermodynamic properties such as the supersaturations while having differences in dipole moment and polarizability. Three of them have very similar molecular structure with the only difference being in the moiety at the end of the long CH chain.

TABLE 2: Physical Chemical Properties of the Working Fluids

	MW	boiling point (°K)	saturation vapor pressure at 20 C (Pa)	solubility in water (ppm (wt))
DBP	278.3	613.15	6.90×10^{-4}	10.8
octadecanoic acid	284.5	648.35	1.57×10^{-4}	2.9
octadecanol	270.5	608.15	1.29×10^{-4}	0.0011
octadecane	254.5	589.86	1.24×10^{-2}	0.0021

Experimental Procedure and Data Reduction

The typical experiment consisted of several steps. In the first step, the parameters of the particle generator were set to produce the desired size nuclei. Typical values of generator temperatures, as well as the vapor flow values, are presented in Table 1 for each different composition of the nuclei. Attention was paid to maintain the mean size of nuclei distributions in the range of 3−10 nm. Particles smaller than 3 nm require very high supersaturations for nucleation. At such a supersaturation, homogeneous nucleation may take place along with the heterogeneous nucleation.[15] Our prior results have made it possible to clearly identify the onset of homogeneous nucleation. Nuclei bigger than 10 nm are well above the expected Kelvin diameters. Thus, sizes around 10 nm were selected so that the details of the onset of heterogeneous nucleation can be studied.

The requirements for number concentration were not as stringent. Number concentrations of $\sim 10^6$ allow good measurement of the electrical current in the Faraday cup of DMA, while keeping coagulation negligible for nucleation and measurement times of a few seconds. The experiments were conducted with limited quantities of the condensable vapor so that the particles did not all activate and grow to a uniform size as would be typically done in a condensation nucleus counter. Thus, the size distributions of activated and partially grown particles were measured to explore the features of these processes.

The geometry of this system including the expanding jet emerging into the condenser makes the calculation of the heat and mass transfer in this system very difficult. Thus, the supersaturation values cannot be estimated, and detailed comparisons with theoretical calculations are not yet possible.

Results and Discussion

The initial size distributions of Ag and NaCl particles are presented in Figure 3. Size distribution measurements are performed with DMA directly after the generator (dir), no flow through the saturator, flow through dry side only ($Q = 0$). The lines represent a log-normal distribution fits to the data. Distributional parameters (median size, d_{50} (nm), and geometric standard deviation, σ_g) are shown in the legend. The size distribution after TMCNC with zero vapor flow is normalized for dilution by the generator flow. As can be seen in Figure 3, the size distribution does not change with or without vapor generator flow. The difference in the size distributions directly after the particle generator and after the TMCNC with/without vapor flow can be explained by diffusional losses in TMCNC and communication lines. In all of the presentations of results, the size distribution with zero vapor flow was used as a reference

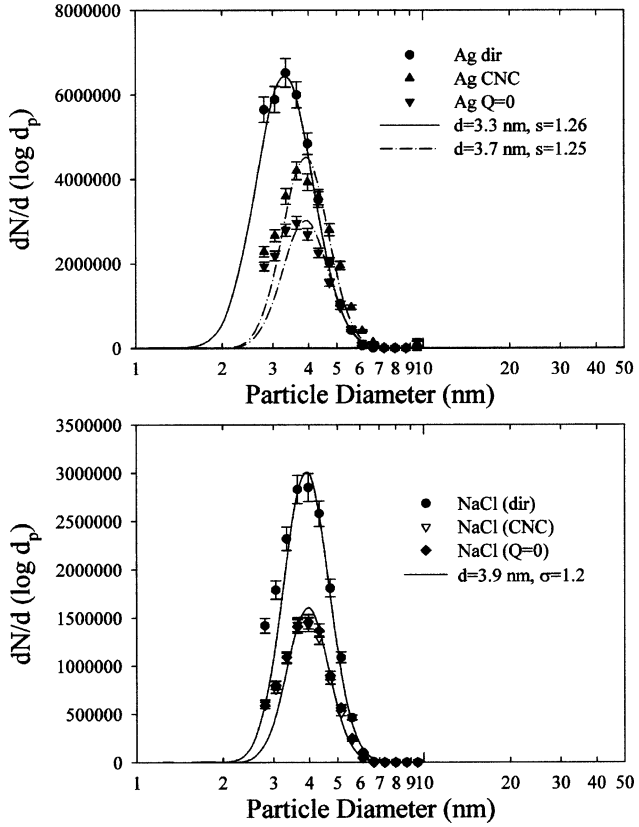

Figure 3. Size distribution of Ag (top) and NaCl (bottom) particles directly after generator (dir), after passing through CNC without vapor generator flow (CNC) and through CNC without vapor flow ($Q = 0$). Lines represent log-normal distribution with parameters shown in the legend, accordingly, number concentration, median size d_{50} (nm) and distribution width σ_g.

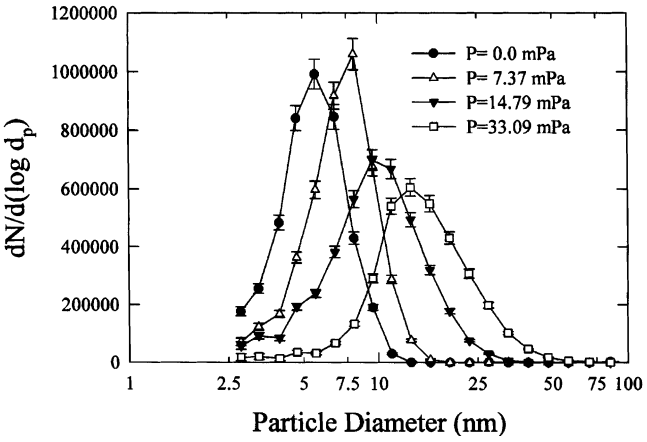

Figure 4. Size distribution of NaCl particles at various pressure of stearic acid vapor.

so that the effect of diffusional loss could be excluded from consideration.

The size distribution changes dramatically when a working fluid vapor is introduced. Figure 4 shows the nucleation of octadecanoic acid on NaCl particles. It can be seen that, as the pressure of the acid increases, the size distribution smoothly increases to larger sizes. In this case, the particles are bigger than their Kelvin diameters so that they activate and grow. The dispersion of the distribution increases with increasing vapor concentration so it appears that the initially larger particles in the distribution grow more rapidly than the smaller particles. The quantity of vapor was deliberately set to be lower than

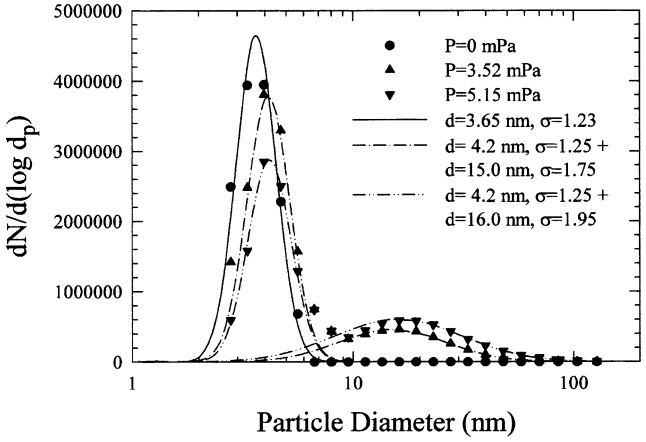

Figure 5. Size distributions of Ag particles as the octadecanol vapor concentration increases. The size distribution can fit to two log-normal distributions.

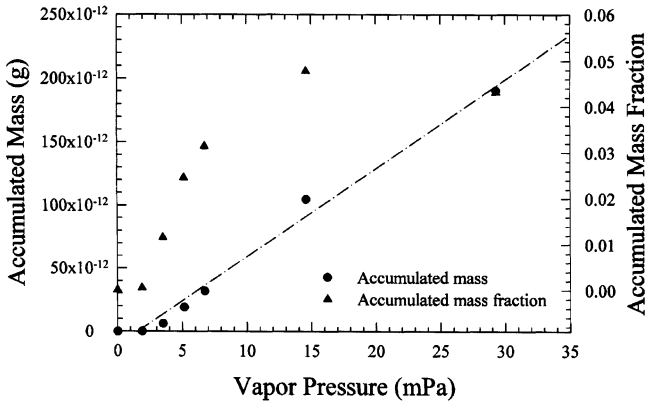

Figure 6. Octadecanol mass accumulated by Ag particles and the accumulated fraction which is the ratio of octadecanol mass accumulated on particles to total mass of octadecanol vapor delivered into system is plotted as a function of the octadecanol partial pressure.

would be needed to permit all of the particles to grow to uniform size as would be typically done in a condensation nucleus counter.

To ensure that there was no production of ion-induced particles in the radioactive charger, experiments were performed with no added particles. Experiments were performed in which (1) there is vapor ($P = 69$ mPa) with no particles observed in the Faraday cup and (2) a higher pressure of vapor ($P = 926$ mPa) with still no observed particles. At these partial pressures of added vapor that are high compared to the other experiments, there were no measured concentrations of particles showing that ion-induced nucleation is not occurring in the system. Similar nucleation and growth patterns are observed for the nucleation of octadecanoic acid on Ag particles, and thus, these results are not shown. Experiments were not performed for KCl or AgCl particles.

Different behavior was observed with the other working fluids. Figure 5 shows the size distributions of Ag particles with increasing octadecanol vapor concentration. A second mode appears in size distribution. The measured size distribution was fit to a bimodal log-normal distribution with the parameters shown in legend. In this case, not all of the particles are activated. Those nuclei that are activated grow into the larger size mode while others remain in a mode that is similar to the generated size distribution.

Figure 6 shows the dependence of octadecanol mass accumulated by Ag particles on pressure of the vapor present in

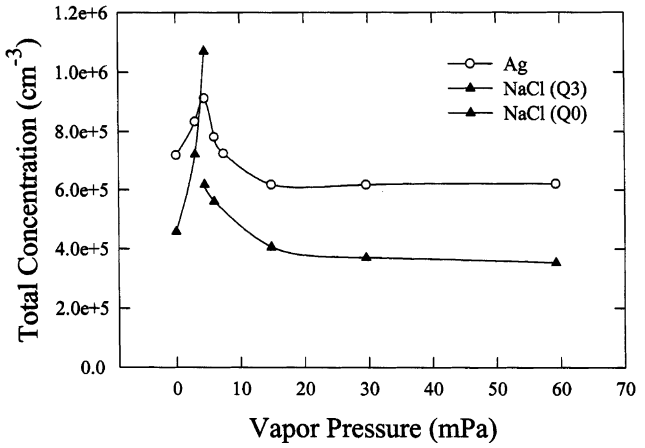

Figure 7. Total number concentrations of particles measured with DMA's Faraday cup electrometer for Ag and NaCl nuclei are plotted against the octadecanol partial pressure.

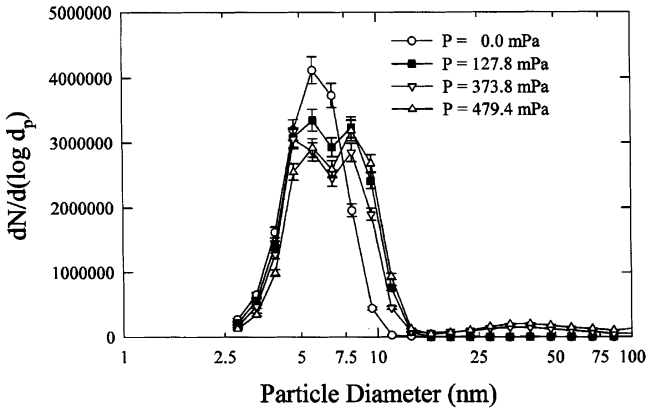

Figure 8. Size distributions of NaCl particles for various octadecane vapor concentrations.

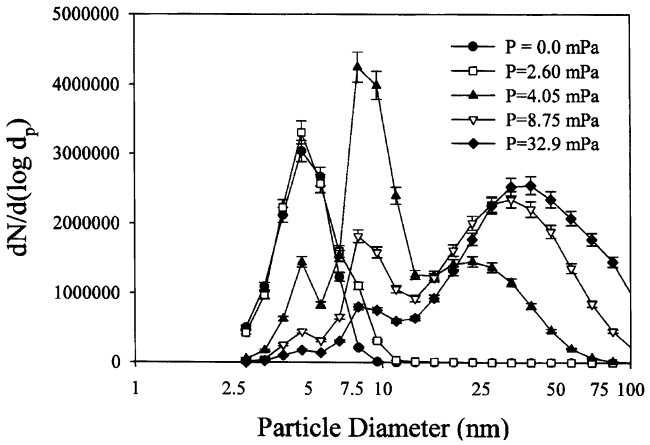

Figure 9. Size distributions of NaCl particles with increasing octadecanol pressure. The size distribution can be fit to three log-normal distributions.

the system. The accumulated fraction shows the ratio of octadecanol mass accumulated on particles to mass of octadecanol vapor delivered into system. The partial pressure and delivered octadecanol mass are estimated using the saturation temperature and wet/dry flow ratio. Prior work has shown that this approach gives good estimates of the vapor present in the system.[14] At low partial pressures, the accumulated liquid ratio increases rapidly with increasing pressure. A strong dependence of the accumulated mass on pressure of the vapor would be expected for the onset of heterogeneous nucleation when the supersaturation is comparable with the critical supersaturation. The accumulated vapor fraction becomes constant at higher pressures since the supersaturation is substantially higher than critical supersaturation and the growth then depends linearly on pressure of the condensable vapor.

The dependence of total number concentration of grown particles on octadecanol vapor pressure is presented in Figure 7. As the working fluid vapor pressure increases, the total particle concentration appears to increase and then decline. This kind of dependence was observed in most experiments. The observed increase in concentration at low vapor concentrations may be due to the diffusional loss of particles in the TMCNC or to their failure to be detected because their size was below the critical size that will activate at the given supersaturation. With the introduction of vapor and beginning of heterogeneous nucleation, the size distribution of nuclei shifts toward larger sizes, reducing the diffusional losses and increasing the detection efficiency. At higher vapor pressures, the grown particles may experience inertial loss or become bigger than the upper detection limit of the DMA, causing the observed reduction of total concentration. Similar behavior is observed for nucleation of dibutylphthalate on NaCl particles (not shown) and for octadecanol on AgCl (not shown).

Quite different results were observed for octadecane and octadecanol vapor nucleation on NaCl nuclei (Figures 8 and 9, respectively). With the introduction of the vapor, the initial unimodal distribution separates into two size modes. However, as additional vapor is added, the distribution does not shift to larger sizes. Instead, a third, much larger size mode appears in the size distribution at high vapor pressures. It may be that these nuclei have several different types of nucleation sites. The second mode may represent accumulation of vapor on the NaCl nuclei, but without heterogeneous nucleation resulting in complete surface coverage of the nucleus. The third mode appears when heterogeneous nucleation begins to fully cover the particle surface. Smorodin[22] has suggested a process of thermodynamic instability in which just such a transition from partial wetting of insoluble particles can occur for increasing concentrations of condensable vapor. The process results in filling the uncovered surface in a "quasi-cavitation process" that can occur at some critical saturation and lead to a sharp growth of the drop. Such a process may be occurring for some of the particles resulting in sufficient reduction in vapor pressure that some particles remain in the initial two modes. These results show the difference between the octadecanoic acid that would be expected to wet the NaCl surface and octadecanol and octadecane that would not be anticipated to wet the surface.

For the octadecanol case, the size distribution was fitted to three log-normal distributions (see Figure 10). Once octadecanol vapor is added and the second mode is formed, the ratio of intensities of these two smaller modes does not change with increasing octadecanol pressure indicating the stability of the two smaller modes. The third mode increases in intensity with increasing vapor such that the ratio of the third mode to the sum of first two increases with an increase of vapor pressure as would be expected in condensational growth. This effect can be seen in Figure 11, parts a and b. Figure 11b shows the dependence of third mode fractions defined as "grown mode" on octadecanol vapor pressure. The "grown mode" fraction increases with octadecanol vapor pressure essentially independently of the initial nucleus size. Similar behavior for modes 1 and 2 was observed in the octadecane/NaCl system.

The increase of "grown mode" fraction with octadecanol vapor pressure can be understood because the increase of

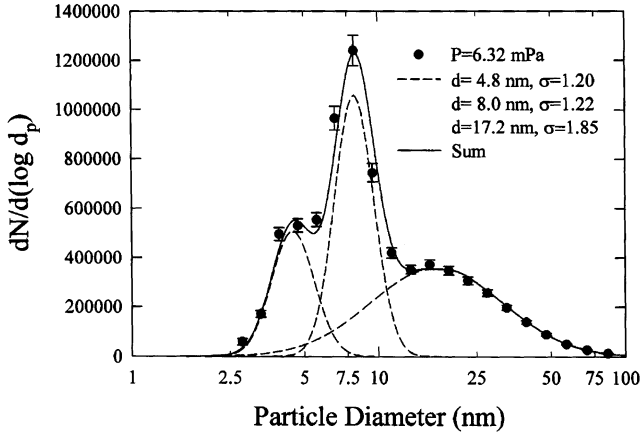

Figure 10. Example of trimodal log-normal fit for a size distribution of particles measured after heterogeneous nucleation of octadecanol vapor on NaCl nuclei. Individual distributions are shown together with experimental data (open circles) and resulting distribution (solid line).

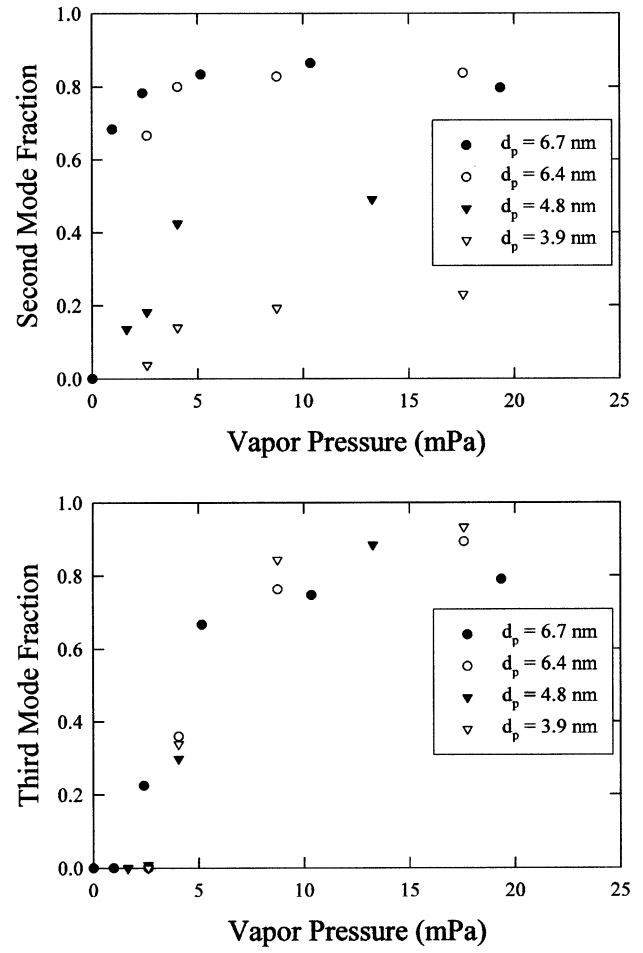

Figure 11. (a) Dependence of second mode fraction ("split mode") on octadecanol vapor pressure. The legend shows initial nuclei size. (b) Dependence of third mode fraction ("grown mode") on octadecanol vapor pressure. The legend shows initial nuclei size.

octadecanol partial pressure increases the supersaturation. With an increased supersaturation, the Kelvin diameter decreases, and more particles should activate and grow. The lack of influence of initial nuclei size is not clear and requires further research.

Figure 11a shows the dependence of the fraction of the second mode ("split mode") on octadecanol vapor pressure. The legend shows the initial nuclei size. It can be clearly seen that the "split mode" fraction does not depend on octadecanol vapor pressure

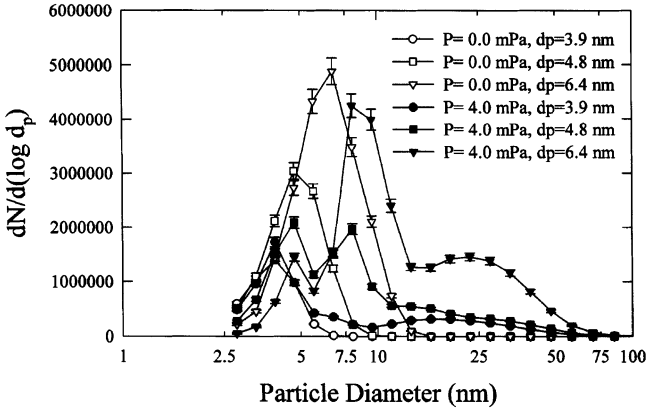

Figure 12. Size distribution of NaCl particles with different initial size distribution at octadecanol vapor pressure of 4 mPa. Initial size distribution of particles also presented (open points). Initial distribution of particles "splits" on line corresponding to 4.8 nm creating trimodal size distribution.

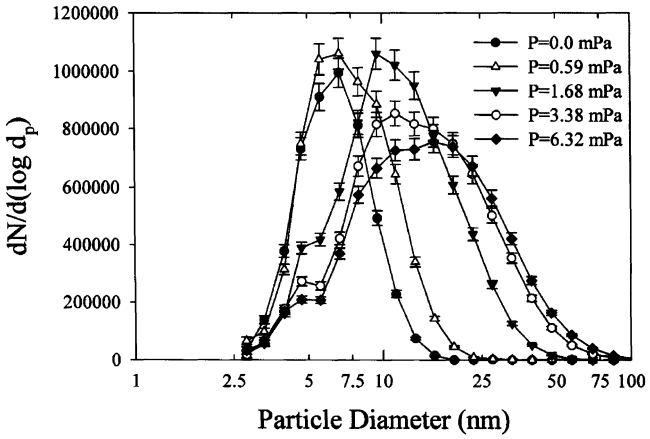

Figure 13. Transformation of size distribution of KCl particles with increase of octadecanol vapor pressure at vapor generator temperature of $T = 75$ °C. Air is used as a carrier gas.

TABLE 3: "Split Mode" Size for Various Conditions

	initial nuclei size, nm	width of distribution	second mode fraction	corresponding size, nm
		Octadecanol		
NaCl	3.9	1.21	0.23	4.5
NaCl	4.8	1.25	0.5	4.8
NaCl	5.4	1.35	0.66	4.8
NaCl	6.4	1.35	0.83	4.8
NaCl	6.7	1.36	0.86	4.7
KCl	4.8	1.3	0.15	6.3
KCl	8.6	1.45	0.8	5.3
		Octadecane		
NaCl	5.7	1.29	0.41	6.0
NaCl	6.2	1.30	0.49	6.3

at values above 5 mPa, but it strongly depends on the initial nucleus size. Another view of the phenomenon can be seen in Figure 12, which shows the size distribution of NaCl particles with different initial size distributions at a fixed octadecanol vapor pressure of ~4 mPa. The initial size distribution of particles is also presented. The initial distribution of particles "splits" at a size corresponding to 4.8 nm to create the trimodal size distribution. Table 3 shows the parameters characterizing the initial size distributions of NaCl nuclei and the corresponding "split mode" fractions. For octadecanol nucleation on NaCl particles, this size is 4.8 nm. A fraction of the nuclei with diameters larger than 4.8 nm increases to 8 nm and remains at this size with increasing octadecanol pressure unless there is a

process that permits them to grow to 15−25 nm. It appears that particles smaller than 4.8 nm do not change their size.

To further explore the nucleation of octadecanol on simple salts, KCl nuclei were used. Figure 13 shows that octadecanol nucleates on KCl nuclei and generally grows in the same manner as it does with the other materials (Ag and AgCl). There is some indication of the formation of the intermediate size mode in Figure 13, but at high pressures of the condensing vapor, this intermediate size mode merges into the grown mode. There were also several experiments of the nucleation behavior of octadecanol on KCl performed in nitrogen as the carrier gas instead of air to ascertain any effects of the carrier gas. The behavior is the same as in air. Similarly, octadecanol on NaCl shows the same trimodal behavior in nitrogen that is essentially identical to the behavior observed in air. Theoretical study of this unusual behavior is clearly needed.

Conclusions

A novel turbulent mixing CNC was developed capable of easily changing the supersaturation values. Three different patterns of nucleation and growth were observed. In the case of octadecanoic acid, all of the nuclei were activated and could then grow as they accumulated vapor. The activation of these nuclei did not appear to be dependent on the composition of the nucleus. For octadecane, octadecanol, and dibutylphthlate, a bimodal pattern was observed for all of the nuclei except the case of octadecanol on NaCl. In this case, some nuclei activate and grow while the remaining particles keep their initial size distribution. In the case of octadecanol and NaCl, a second mode only slightly larger than the initial size distribution forms in the presence of even small amounts of vapor. When the partial pressure of octadecanol reaches a sufficiently high value, some of the nuclei activate into a grown mode. It appears nucleation occurs on both of the smaller modes in equal proportion as the relative intensity of the two smaller modes remains unchanged as the vapor concentration is increased. Further study of these phenomena and a careful theoretical evaluation are now required to understand the observations presented in this report.

Acknowledgment. This work is supported by U.S. Environmental Protection Agency under Grant R826654. We acknowledge the useful discussions of these results with Professor Michael Anisimov of Clarkson University and Prof. Vladimir Smorodin of Moscow State University.

References and Notes

(1) Oberdörster, G.; Ferin, J.; Lehnert, B. E. *Environ. Health Perspect.* **1994**, *102*, (Suppl 5) 173.

(2) Wichmann, H.-E.; Spix, C.; Tuch, T.; Wolke, G.; Peters, A.; Heinrich, J.; Kreyling, W. G.; Heyder, J. Daily mortality and fine and ultrafine particles in Erfurt, Germany. Part I: role of particle number and particle mass. Health Effects Institute: Cambridge, MA, 2000; Research Report no. 98.

(3) Helsper, C.; Niessner, R. *J. Aerosol Sci*. **1985**, *16*, 457.

(4) Porstendörfer, J.; Scheibel, H.; Pohl, F.; Preining, O.; Reischl, G.; Wagner, P. *Aerosol Sci. Technol.* **1985**, *4*, 65.

(5) Kousaka, Y.; Okuyama, K.; Niida, T. In *Aerosols*; Liu, B., Pui, D., Fissan, H., Eds.; Elsevier: New York, 1984; p 51.

(6) Madeline, G., Metayer, Y. *J. Aerosol Sci.* **1980**, *11*, 358.

(7) Holländer, W.; Dunkhorst, W.; Windt, H. In *Nucleation and Atmospheric Aerosols 2000*; AIP Conference Proceedings No. 534; American Institute of Physics: College Park, MD, 2000; pp 732−735.

(8) Kulmala, M.; Lauri, A.; Vehkamäki, H.; Laaksonen, A.; Petersen, D.; Wagner, P. E. *J. Phys. Chem. B* **2001**, *105*, 11800.

(9) Chen, C.-C.; Huang, C.-C.; Tao, C.-J. *J. Colloid Interface Sci.* **1999**, *211*, 193.

(10) Chen, C.-C.; Tao, C.-J. *J. Chem. Phys.* **2000**, *112*, 9967.

(11) Chen, C.-C.; Tao, C.-J.; Shu, H.-J. *J. Colloid Interface Sci.* **2000**, *224*, 11,

(12) Chen, C.-C.; Tao, C.-J.; Huang, C.-C. *J. Colloid Interface Sci.* **2002**, *255*, 158.

(13) Hogrefe, O. V.; Keesee, R. G. *Aerosol Sci. Technol.* **2002**, *36*, 239.

(14) Lee, D.-W.; Hopke, P. K.; Mavliev, R.; Wang, H. C. *J. Phys. Chem. B* **2003**, *107*, 13813.

(15) Mavliev, R.; Hopke, P. K.; Wang, H.-C.; Lee, D.-W. *Aerosol Sci. Technol.* **2001**, *35*, 586.

(16) Fissan, H.; Hummes, D.; Stratmann, F.; Buscher, P.; Neumann, S.; Pui, D. Y. H.; Chen, D. *Aerosol Sci. Technol.* **1996**, *24*, 1.

(17) Rossel-Llompart, F.; Losceratales, I.; Bingham, D.; Fernandez de la Mora, J. *J. Aerosol Sci.* **1996**, *27*, 695.

(18) Stolzenburg, M. R.; McMurry, P. H. *Aerosol Sci. Tech.* **1991**, *14*, 48.

(19) Reischl, G. P.; Makela, J. M.; Necid, J. *Aerosol Sci. Technol.* **1997**, *27*, 651.

(20) Reisch, G. P. *Aerosol Sci. Technol.* **1991**, *14*, 5.

(21) Leong, K. H.; Hopke, P. K.; Stukel, J. J. *J. Aerosol Sci.* **1983**, *14*, 23.

(22) Smorodin, V. Ye. *Atmos. Environ.* **1997**, *31*, 1239.